12WCEE 2000

THE EFFECT OF FLEXIBLE HORIZONTAL DIAPHRAGMS ON THE SEISMIC TORSONAL RESISTANCE OF SYSTEMS WITH DUCTILE WALLS

Masahide MURAKAMI[1], Peter J MOSS[2], Athol J CARR[3] And Mashiro INAYAMA[4]

SUMMARY

The roofs and floors of timber houses are often forced to behave as horizontal diaphragms in order to transfer the shear force from the upper storey to the walls of the first storey, particularly when the second storey is set back from the first storey. There has been no way to predict that kinds of damage for seismic assessments of existing buildings up to now. A seismic design procedure for torsional effects on ductile wall systems connected to a rigid horizontal diaphragm has been proposed by T. Paulay. A new design or seismic assessment procedure in which Paulay's torsional model is extended to ductile wall systems connected to flexible diaphragms is presented in this paper. The shear stresses acting on each diaphragm between the walls are estimated by using the difference between the distinct earthquake induced lateral force and the ultimate shear capacity of each wall. The storey drift of each wall is computed by superimposing the local diaphragm shear angles on the overall twist angle of the floor computed assuming a rigid diaphragm. Nonlinear dynamic time history analyses were carried out to verify this design or assessment procedure.

INTRODUCTION

The roofs and floors of timber houses are often forced to behave as horizontal diaphragms in order to transfer the shear force from the upper storey to the walls of the first storey, particularly when the second storey is set back from first storey. Some of the timber houses collapsed in the Hyogoken-Nanbu earthquake in Japan in 1995 because of the lack of shear capacity of their roofs as shown in Photo.1. There is no way to predict that kind of damage for seismic assessments of existing buildings up to now. The objective of this paper is to propose an idea to predict the damage of timber houses whose second storey is set back from the first storey via weak roofs or floors.

The seismic design procedure for the torsional effects on ductile wall systems connected to a rigid horizontal diaphragm has been proposed by T. Paulay[1997]. A new design or seismic assessment procedure in which Paulay's torsional model is extended to ductile wall systems connected to a flexible diaphragm is presented in this paper.

PROPOSED DESIGN AND /OR ASSESSMENT PROCEDURE

2.1. Torsional Behaviours of Ductile Wall Systems with Rigid Diaphragms

The seismic design procedure for the torsional effects on ductile wall systems connected to a rigid horizontal diaphragm has been proposed by T. Paulay as shown in Fig.1, where the shear force - storey drift relationship of a wall system is assumed to be bi-linear in this theory. The earthquake induced lateral force, which is balanced with the total ultimate shear capacity of a wall system in the Y direction, acts at the centre of mass, CM, in this rigid diaphragm theory. The centre of resistance, CR, means the position of the force line of the total ultimate shear capacity of a wall system in the Y direction. The twist due to the torque occurred by the difference between the centre of mass and the centre of resistance can be restrained only by the elastic rotational stiffness "k_t" carried by a wall system in the X direction when all walls in the Y direction deform beyond the yield

[1] *Dept of Architecture, School of Science & Engineering, Kinki University,Osaka, Japan. Email:murakami@arch.kindai.ac.jp*
[2] *Dept of Civil Engineering, University of Canterbury, Christchurch, New Zealand.*
[3] *Dept of Civil Engineering, University of Canterbury, Christchurch, New Zealand.*
[4] *Inayama Architect, Musahino, Tokyo, Japan.*

displacement because the rotational stiffness of a wall system in the Y direction is zero after yield. The wall displacements are distributed linearly as shown in Fig.2, where "θ_t" is the twist angle calculated by $(\Sigma Q_{ui})e/k_t$, and "e" is the distance between CM and CR. The system displacement in a wall system with a rigid diaphragm is the displacement at the centre of mass. The system displacement can be determined by satisfying the displacement ductility capacity of a critical wall in this wall system.

2.2. Torsional Behaviours of Ductile Wall systems with Flexible Diaphragms

Inertia forces caused by horizontal acceleration are developed throughout a structure as earthquake induced lateral forces. The concept of the distinct earthquake induced lateral force that belongs to each wall is introduced in this calculation procedure. The distinct earthquake induced lateral force can be calculated from the mass supported by each wall as shown in Fig.3 by assuming that uniform horizontal acceleration "a" is exerted to each mass. The total ultimate shear capacity of the wall system in the Y direction is balanced with the total earthquake induced lateral force of the structure. The shear force acting on each local diaphragm between walls can be calculated from the difference between the ultimate shear capacity and the earthquake induced lateral force of each wall, and the distribution of shear forces acting on a diaphragm can be drawn as shown in Fig.4. The equilibrium of moments can be expressed as Eq.(1) by assuming that all walls in the Y direction yield completely and that all walls in the X direction stay in the elastic range.

$$k_t \cdot \theta_t + \sum (P_i - Q_{ui}) \cdot l_i = 0 \qquad (1)$$

The twist angle "θ_t" can be calculated without the calculation of the distance between CM and CR, "e", by using Eq.(1). Eq.(1) can be derived by making a linear elastic analysis of a statically determinate structure as shown in Fig.5. Flexural deformation is neglected in this procedure because shear deformation is larger than flexural deformation when a flexible diaphragm is deformed. The local diaphragm shear stress "τ_{ij}" can be calculated as shown in Fig.5. The local diaphragm shear angle is given by $\gamma=\tau/G$ (γ: engineering shear strain, G: shear stiffness). The storey drift of each wall is computed by superimposing the local diaphragm shear angles on the overall twist angle of the diaphragm computed assuming a rigid diaphragm as shown in Fig.6.

The system displacement can be represented as the average displacement of the wall system in the Y direction because the displacement at the centre of mass may depend on the shear deformation of a local diaphragm adjacent to the centre of mass.
In actual buildings, the number of walls is larger than the example shown in Fig.5 and the shape of a diaphragm is more complicated. The procedure of modelling a statically determinate structure is as follows in these cases;

(1) Walls in the X direction are modelled into elastic springs supported with rollers.
(2)A diaphragm is modelled into truss elastic elements or quadrilateral elastic finite elements supported at one node, i.e. one wall in the Y direction, with a roller in the Y direction.
(3) Induced forces "P_i-Q_{ui}" in the Y direction are applied to the other walls. Then the shear stress acting on each diaphragm, the shear force acting of each wall in the X direction, and relative displacement of each wall in the Y direction relative to the supported node can be determined by a linear elastic analysis.

3.VERIFICATION WITH TIME HISTORY ANALYSES

3.1 Parameters of Numerical Studies

Time history analyses with two different kinds of structures were carried out to verify this simple design and/or assessment procedure. The parameters for the numerical studies are shown in Table 1. The model code "AXXX", where the symbol "X" indicates any symbol in Table (a), are the structures in which the shear stiffness and ultimate shear capacity of Frame 3 are the largest and those of Frame 2 are the smallest. "ARXX" are the structures with a rigid diaphragm. "ASXX" are the structures with a flexible diaphragm. The displacement of Frame 2 of "ASXX" is larger than that of "ARXX". There is no wall at the position of Frame 1 in "BXXX", therefore the displacements at Frame 1 are the largest due to twist. The Stewart degrading stiffness hysteresis rule[1987] is used for all springs except "k_{y3}" in "XXXB" as illustrated in the inset figure in Table 1. The yield displacement "dy" and the ultimate displacement "du" of all springs have the same values in the structures "XXXU". The values of "dy" and "du" of "k_{y3}" are larger than those of "k_{y1}" and "k_{y2}" in the structures "XXXS". The Stewart hysteresis rule is used for "k_{y1}" and "k_{y2}" and the bi-linear hysteresis rule is used for "k_{y3}" in the structures "XXXB". The parameters for the base shear coefficients and excitations are given in Table 1. 5% initial stiffness Rayleigh damping is used throughout these numerical studies.

The response of a single degree of freedom (SDOF) system concerned to each model was computed as follows:
The tri-linear envelope curves of the Stewart hysteresis rule in the SDOF system "XXXU" and "XXXS" are determined by making their dissipated energies equal to those of the total envelope curves of "k_{y1}","k_{y2}", and "k_{y3}". The co-ordinates of the envelope curve of "XXXU" are (dy=2.5cm, Fy=2000kgf) and (du=5cm, Fu=3000kgf), and those of "XXXS" are (dy=2.55cm,Fy=2000kgf) and (du=5.1cm,Fu=3000kgf). The springs "k_{y1}","k_{y2}", and "k_{y3}" are connected in parallel at the centre of mass in the SDOF system "XXXB". The total yield shear capacity and the total ultimate shear capacity in the Y direction are the same values throughout these numerical studies. The total shear capacities of "XX3X" in the X direction are 75% of those in the Y direction, and those of "XX6X" in the X direction are 150% of those in the Y direction.
The characteristics of twist calculated by linear static analyses mentioned above are shown in Fig.7 where relative displacements against Frame 2 are plotted. Frame 2 is supported with a roller in the Y direction and elastic stiffnesses "k_o" are used for "k_x". The order of local diaphragm shear angles "γ" is similar to that of the twist angle of a rigid diaphragm "θ_t" when a diaphragm is flexible.

3.2 Prediction of System Displacements from Responses of SDOF Systems

The typical time histories of the averaged displacement of Frames 1, 2, and 3 compared with the displacement response of the SDOF system are shown in Figs.8 where the model codes are "XXXU" and the ultimate shear coefficients are 0.3. The response waveforms are generally similar to those of SDOF systems. The maximum displacement responses of the SDOF system versus the maximum values of the averaged displacement of Frame 1, 2, and 3 are plotted in Fig.9. Most of the models except a few whose C_{bu} is 0.4 are deformed beyond "du" at the maximum displacement responses. The maximum values of the averaged displacement of Frame 1, 2, and 3 are generally smaller than the maximum displacement responses of the SDOF system as shown in Fig.9.

3.3 Prediction of the Maximum Displacement of Each Frame from the System Displacement

The system displacement "δ_{ave}" can be defined by Eq.(2), where "δ_n" is the maximum displacement response of "Frame n", and $\Delta_1 \ldots \Delta_n$ (Δ_n=0)$\ldots\Delta_i$ are the relative displacements of frames against "Frame n" which is supported by a roller in linear static analysis as shown in Fig.5

$$\delta_{ave} = \frac{1}{i}\sum_{j=1}^{i}(\Delta_j + \delta_n) \tag{2a}$$

$$\delta_n = \delta_{ave} - \frac{1}{i}\sum_{j=1}^{i}\Delta_j \tag{2b}$$

The value of "δ_n" was determined by giving the system displacement "δ_{ave}" which is equal to the maximum of average displacement of Frame 1, 2, and 3 computed with a time history analysis to verify Eq.(2). Then the maximum displacement response of each frame "$\Delta_j+\delta_n$" was found. The maximum displacements of each frame by time history analyses versus the predicted displacement of each frame by the procedure mentioned above are plotted in Fig.10. The main reason for differences between them is due to overestimation of the predicted twist angle of "BSXX" in linear static analyses.

3.4 Prediction of the Maximum Displacement of Each Frame from the Maximum Displacement of SDOF System

The maximum displacement response of each frame "$\Delta_j+\delta_n$" can be calculated from Eq.(2) by giving "δ_{ave}" which is equal to the maximum displacement response of the SDOF system. The maximum displacement of each frame by time history analyses versus the displacement of each frame predicted from the maximum displacement response of the SDOF system by using Eq.(2) are plotted in Fig.11. The errors of Fig.11 are larger than those of Fig.10 because the errors of Fig.11 contain those of Figs.9 and 10. The displacement of each frame predicted from the maximum displacement response of the SDOF system is 1.5 times greater than the maximum displacement response of each frame by time history analysis on the average, and approximately 2.5 times greater on the maximum. It is generally recognised that wide scattering of plots occurs when diaphragms are flexible because the number of degree of freedom of the structures with flexible diaphragms is greater than that of structures with rigid diaphragms.

3.5 Prediction of Shear Forces Acting on Perpendicular Walls and Diaphragms

The maximum shear forces acting on perpendicular walls and diaphragms computed by time history analyses are plotted in Figs.12 and 13 respectively, in which the shear forces predicted based on linear static analyses are

indicated as the lines “Calc.”. All plots are shifted from left to right when the ultimate shear coefficient “C_{ub}“ goes from 0.2 to 0.4 in each group. The mean values and standard deviations of the ratios of shear forces by time history analyses against those by linear static analyses throughout the group “XRXX” or “XSXX” are also shown. It is generally recognised that shear forces acting on perpendicular walls in structures with rigid diaphragms are larger than those with flexible diaphragms. Some plots of “BX3X” reach the ultimate shear capacity “F_u” because the predicted value is larger than “F_u”. The predicted shear forces acting on perpendicular walls are close to the mean value of shear forces computed by time history analyses. The predicted shear forces acting on diaphragms are close to the mean values of computed shear forces acting on diaphragms except the diaphragm between Frame1 and 2 of “AXXX”. It is generally recognised that the plots of structures with flexible diaphragms are more scattered than those of structures with rigid diaphragms because the number of degree of freedom of structures with flexible diaphragms becomes greater than that of structures with rigid diaphragms.

4.CONCLUSION

A seismic assessment procedure to predict torsional behaviour of ductile wall systems with flexible diaphragms has been proposed in this paper.

The displacement of each frame predicted from the maximum displacement response of the SDOF system is 1.5 times greater than the maximum displacement response of each frame by time history analyses on the average, and approximately 2.5 times greater on the maximum.

It is generally recognised that the predicted shear forces acting on perpendicular walls and diaphragms of structures with flexible diaphragms are more scattered than those of structures with rigid diaphragms because the number of degree of freedom of structures with flexible diaphragms becomes greater than that of structures with rigid diaphragms.

The accuracy of this simple procedure is not good enough but these predicted values may be utilized as a tentative criterion by introducing a safety factor after further numerical studies.

REFERENCE

T.Paulay (1997), “Seismic Torsional Effects on Ductile Structural Wall System”, *Journal of Earthquake Engineering*, Vol.1, No.4, Imperial College Press, pp.721-745

W.Stewart (1987), The Seismic Design of Plywood Sheathed Shear Wall, Phd. Thesis, University of Canterbury, New Zealand

ACKNOWLEDGEMENT

The authors would like to thank T.Paulay, Emeritus Professor of University of Canterbury, for his advice.

Original shape of collapsed house

Deformation of flexible diaphragm

A collapsed house due to weak roof at Kobe in 1995 This type of NZ house may have a similar problem.

Photo. 1: Problems of flexible diaphragms

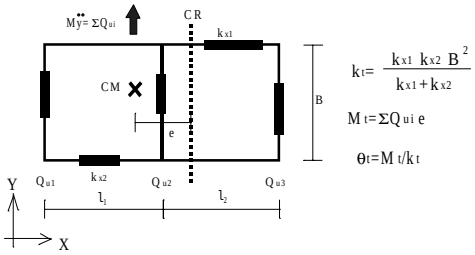

Figure 1: Rigid diaphragm theory

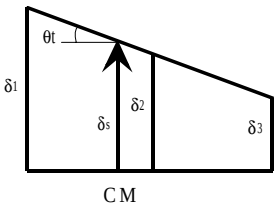

Figure 2: Deformation pattern of rigid diaphragm theory

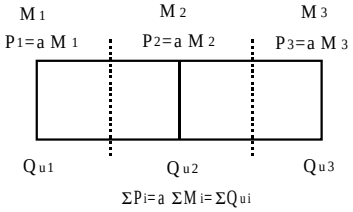

Figure 3: Distinct earthquake induced lateral forces

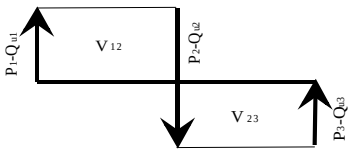

Figure 4: Shear force distribution

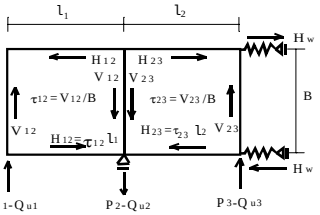

Figure 5: Analytical model pattern

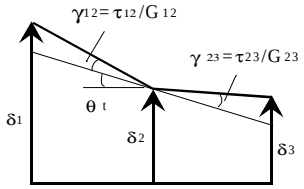

Figure 6: Modified displacement

Table 1: Parameters of numerical studies

(a) Definition of model code

Symbol	A B	R S	3 6	U S B
Ref. Table No.	(b)	(c)	(d)	(e)

(b) Strengths of springs in Y direction

Sym-bol	Spring arrangement	ky1(kgf)		ky2(kgf)		ky3(kgf)	
		Fy	Fu	Fy	Fu	Fy	Fu
A	Type A	700	1050	200	300	1100	1650
B	Type B	0	0	1000	1500	1000	1500

(c)Elastic stiffnesses of diaphragm springs

Symbol	G(kgf/cm)
R	1000000 (rigid)
S	100 (flexible)

(d) Characteristics of springs in X direction

Symbol	ko	Fy	dy	Fu	du
3	300	750	2.5	1125	5
6	600	1500	2.5	2250	5

Hysteresis =W.Stewart model unit:kgf, cm

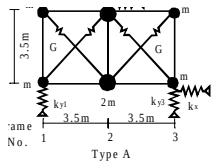

Type A

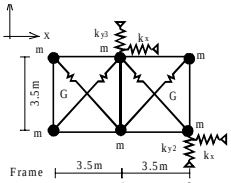

Type B

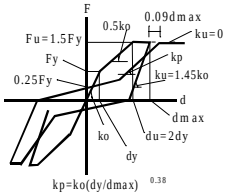

W.Stewart model

Base shear coefficient at ultimate state=0.2, 0.3, 0.4

Excitations in Y direction (Vmax=50cm/s (50kine))
El.Centro 1940 NS, Taft EW, Kobe NS, Hachinohe NS

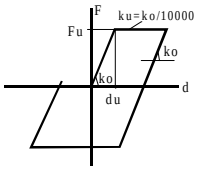

Bi-linear model

(e) Displacement and hysteresis rules

Symbol	ky1			ky2			ky3		
	Model	dy	du	Model	dy	du	Model	dy	du
U	S	2.5	5	S	2.5	5	S	2.5	5
S	S	2	4	S	2	4	S	3	6
B	S	2	4	S	2	4	B	3	4.5

S=W.Stewart model, B=Bi-linear model unit:cm

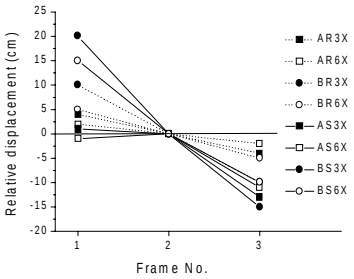

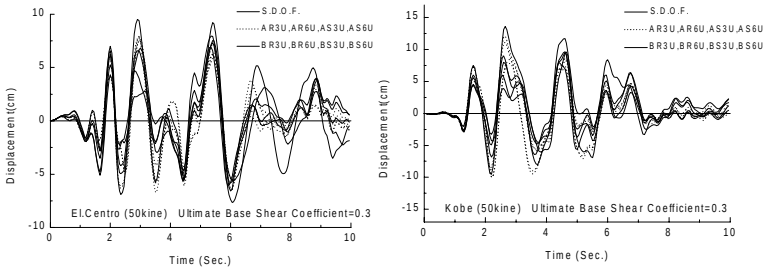

Figure7: Static characteristics **Figure8: Typical displacement time histories**

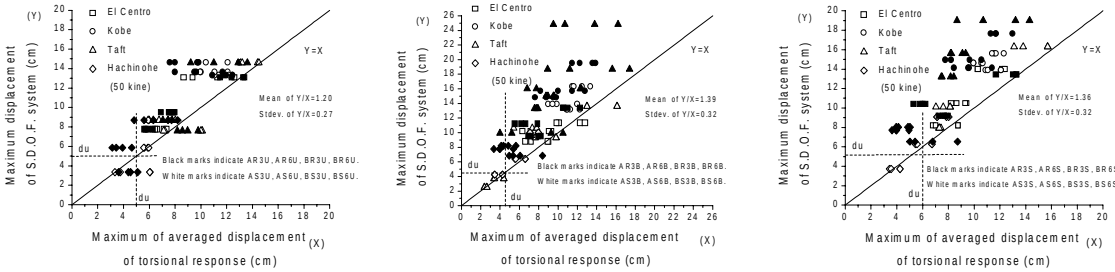

(a) XXXU (b) XXXS (c) XXXB

Figure9: Prediction of system displacements

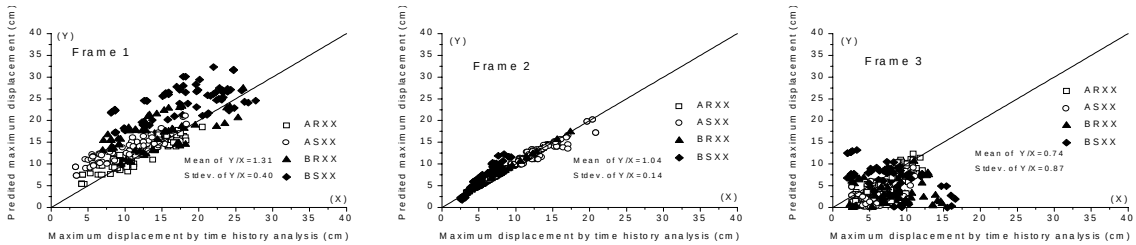

Figure10: Prediction of maximum displacement of each Frame from system displacement

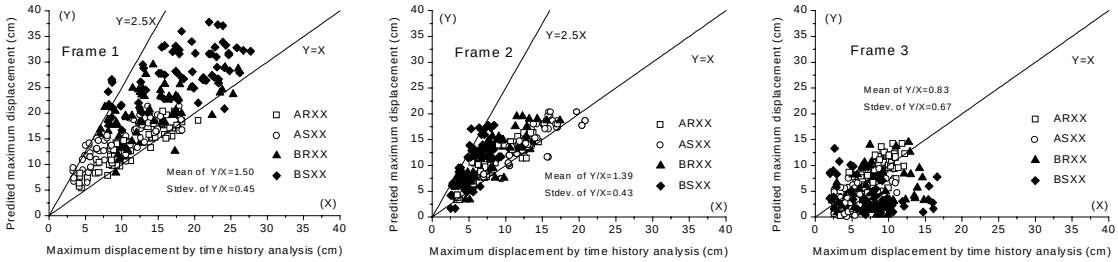

Figure11: Prediction of maximum displacement of each Frame from response of SDOF system

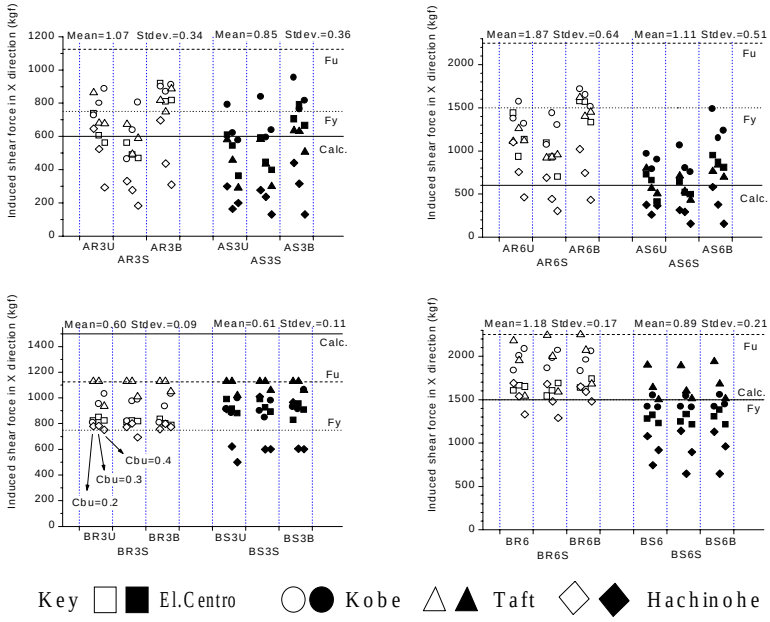

Figure12: Shear forces of perpendicular walls

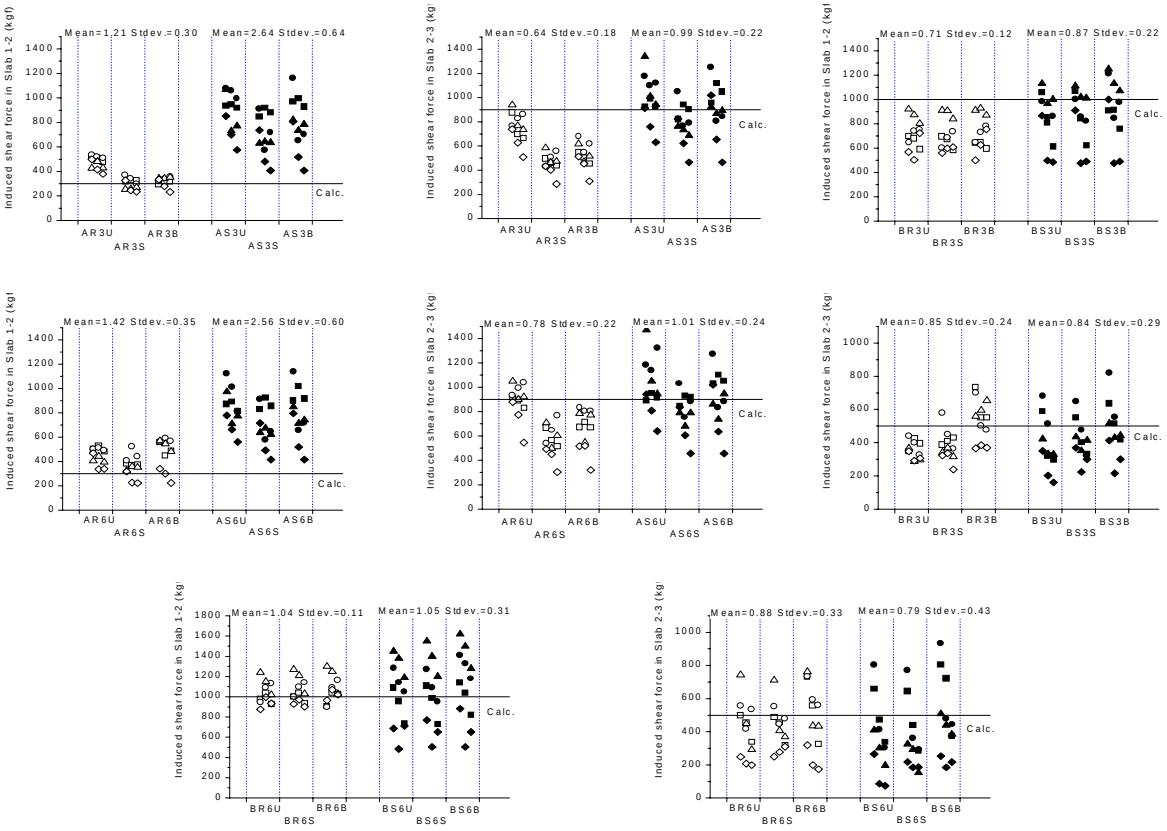

Figure13: Shear forces acting on diaphragms